Letter

Large deviations in chaotic systems: Exact results and dynamical phase transition

Naftali R. Smith [*]

Department of Solar Energy and Environmental Physics, Blaustein Institutes for Desert Research, Ben-Gurion University of the Negev, Sede Boqer Campus, 8499000, Israel

(Received 10 April 2022; accepted 19 September 2022; published 20 October 2022)

Large deviations in chaotic dynamics have potentially significant and dramatic consequences. We study large deviations of series of finite lengths N generated by chaotic maps. The distributions generally display an exponential decay with N, associated with large-deviation (rate) functions. We obtain the exact rate functions analytically for the doubling, tent, and logistic maps. For the latter two, the solution is given as a power series whose coefficients can be systematically calculated to any order. We also obtain the rate function for the cat map numerically, uncovering strong evidence for the existence of a remarkable singularity of it that we interpret as a second-order dynamical phase transition. Furthermore, we develop a numerical tool for efficiently simulating atypical realizations of sequences if the chaotic map is not invertible, and we apply it to the tent and logistic maps.

DOI: 10.1103/PhysRevE.106.L042202

Introduction. Classical chaos is a fundamental property of a host of natural systems. It describes the unpredictability of deterministic dynamical systems, due to exponential growth of uncertainties in the initial conditions—the "butterfly effect." This notion gives rise to effective statistical descriptions of chaotic systems that form the foundations of statistical mechanics, for example, in terms of standard or anomalous diffusion [1–5]. Rare events (large deviations) in chaotic dynamics can be extremely important, as they can have significant and potentially catastrophic consequences. One important example is extreme weather events such as heat waves or floods [6–12], whose probabilities are especially challenging to predict under today's changing climate conditions which preclude using only historical data to assess their likelihood. Additional examples are found in dynamics of stock markets [13], road traffic [14], populations [15–17], and pandemics [18].

However, while large deviations in stochastic systems have been extensively studied, both theoretically and numerically [19–46], large deviations in deterministic, chaotic systems have received somewhat less attention (see, however, Refs. [6–12,16,47–63]). In particular, for chaotic systems there are fewer existing exact analytic results for the rate (large-deviation) function, which is a central object in the study of large deviations (see the definition below). Of particular interest are dynamical phase transitions (DPTs): singularities of rate functions that lead to distribution tails that are much larger or much smaller than one would naively expect.

In principle, one would not expect there to be a fundamental difference between the large-deviation behaviors of chaotic and stochastic systems, because symbolic dynamics maps chaotic systems to stochastic ones. However, it is usually not straightforward to give explicit symbolic dynamics, so it is not always easy to apply methods that work for stochastic systems to chaotic ones. In numerical Monte Carlo (MC) simulations, these difficulties are usually circumvented by adding a weak noise term [6,7,64], although alternatives exist [65].

Let us define the class of problems that we study here. We consider a sequence $\boldsymbol{x}_1, \dots, \boldsymbol{x}_N$ of elements of $\mathbb{R}^d$ generated by a chaotic map $f(\boldsymbol{x})$ via $\boldsymbol{x}_{i+1} = f(\boldsymbol{x}_i)$, where $\boldsymbol{x}_1$ is randomly sampled from the invariant measure (IM) of the process $p_s(\boldsymbol{x})$. We recall that the IM is the measure that is preserved by the map $f(\boldsymbol{x})$, i.e., if $\boldsymbol{x}$ is distributed according to the IM, so is $f(\boldsymbol{x})$. We quantify fluctuations in the system by studying the full distribution of dynamical observables

$$A = \frac{1}{N}\sum_{i=1}^{N} g(\boldsymbol{x}_i), \tag{1}$$

where $g : \mathbb{R}^d \to \mathbb{R}$. The study of dynamical observables has been an important theme in the ongoing research of large deviations, and importantly for the following, it is amenable to theoretical analysis via the powerful Donsker-Varadhan (DV) formalism [19,23,27,43,44]. The DV theory is more commonly formulated for stochastic systems, however, its formulation for chaotic systems is straightforward and has been known for some time [55,66,67]. Note that A is a deterministic function of the initial condition $A = \mathcal{A}(\boldsymbol{x}_1)$. In the large-$N$ limit, for ergodic dynamics, A converges to its ensemble-average value $A \to \int g(\boldsymbol{x}) p_s(\boldsymbol{x}) d\boldsymbol{x} \equiv a_*$ with probability 1. Individual realizations, however, deviate from this value due to fluctuations in the initial condition $\boldsymbol{x}_1$. For the particular case $g(\boldsymbol{x}) = \ln |J_f(\boldsymbol{x})|$, where J_f is the Jacobian determinant [68,69], A corresponds to the finite-time Lyapunov exponent [48–54,56–63,66], which describes the rate of separation with respect to nearby trajectories over a finite time.

The DV framework predicts that, under fairly general conditions, fluctuations obey a large-deviation principle (LDP)

[*]naftalismith@gmail.com

[27,55,66,67,70]

$$P(A=a) \sim e^{-NI(a)}, \quad N\to\infty, \tag{2}$$

where $I(a) = -\lim_{N\to\infty} \frac{\ln P(A=a)}{N}$, the "rate function," encodes the system's dynamical behavior. $I(a)$ is convex and vanishes at its minimum, which is at $a = a_*$. Note that in Markov chains (sequences generated by stochastic maps), the initial condition is generally not important because it is quickly "forgotten" as a result of the randomness of the dynamics. In contrast, for a deterministic, chaotic system, *all* of the randomness enters in the initial condition. As has been known for quite some time [27,55,66,67], $I(a)$ can be calculated by solving an auxiliary problem of finding the largest eigenvalue of a "tilted operator" which is related to the generator of the dynamics, which in the present case is the Frobenius-Perron operator. In this Letter, we carry out this calculation explicitly and obtain the exact rate functions $I(a)$ for the doubling, tent, and logistic maps for particular observables [71]. For the cat map, we compute $I(a)$ numerically, uncovering strong evidence for the existence of a remarkable singularity of it that we interpret as a DPT, which signals a sudden change in the way that the system realizes a given value $A = a$ as a crosses the critical point. Furthermore, for noninvertible maps $f(\boldsymbol{x})$, we develop a MC algorithm that efficiently samples realizations that reach unlikely values of A by generating the sequence $\boldsymbol{x}_1,\dots,\boldsymbol{x}_N$ in reverse order and in a biased manner.

Theoretical framework. The theoretical framework that we use to obtain the scaling (2) and calculate $I(a)$ has been known (in various forms) for decades [27,55,66,67], and we recall it here for the sake of completeness. It is useful to first consider the scaled cumulant generating function (SCGF) $\lambda(k)$, defined as $\langle e^{NkA}\rangle \sim e^{N\lambda(k)}$. $\lambda(k)$ is found by calculating the largest eigenvalue of a "tilted" (modified) generator of the dynamics, where $k\in\mathbb{R}$ is the tilting parameter. The existence of a nonzero $\lambda(k)$ yields the scaling (2), and $I(a)$ is then obtained via a Legendre-Fenchel transform [27,66,67] $I(a) = \sup_{k\in\mathbb{R}}[ka - \lambda(k)]$.

We first note that if $\rho(\boldsymbol{x})$ is the probability distribution function (PDF) of some element $\boldsymbol{x} = \boldsymbol{x}_i$, then the PDF of the next element $\boldsymbol{y} = \boldsymbol{x}_{i+1}$ is $L\rho(\boldsymbol{y})$, where L is the Frobenius-Perron operator,

$$L\rho(\boldsymbol{y}) = \int \rho(\boldsymbol{x})\delta(\boldsymbol{y}-f(\boldsymbol{x}))d\boldsymbol{x} = \sum_{z=f^{-1}(y)} \frac{\rho(z)}{|J_f(z)|}. \tag{3}$$

The SCGF $\lambda(k)$ is equal to the logarithm of the largest (real) eigenvalue of the "tilted" operator [21,27,66,67,73,74]

$$L_k\rho(\boldsymbol{y}) = \int e^{kg(\boldsymbol{x})}\delta(\boldsymbol{y}-f(\boldsymbol{x}))\rho(\boldsymbol{x})d\boldsymbol{x} = \sum_{z\in f^{-1}(y)} \frac{e^{kg(z)}\rho(z)}{|J_f(z)|}. \tag{4}$$

Note that $L_{k=0} = L$ whose largest eigenvalue is $e^{\lambda(k=0)} = 1$, the eigenvector being the IM $p_s(\boldsymbol{x})$. It is convenient to define $\psi(\boldsymbol{x}) = e^{kg(\boldsymbol{x})}\rho(\boldsymbol{x})$, so the equation $L_k\rho(\boldsymbol{x}) = e^{\lambda(k)}\rho(\boldsymbol{x})$ becomes

$$\tilde{L}_k\psi(\boldsymbol{x}) = e^{kg(\boldsymbol{x})} \sum_{z\in f^{-1}(x)} \frac{\psi(z)}{|J_f(z)|} = e^{\lambda(k)}\psi(\boldsymbol{x}). \tag{5}$$

The calculation of the full distribution of A is thus mapped to the auxiliary problem of calculating the largest eigenvalue $\lambda(k)$ of the operator $\tilde{L}_k$ [27,55,66,67]. We emphasize that $\lambda(k)$ depends on the observable in question through the function $g(\boldsymbol{x})$ which enters in Eq. (5). As a result, the rate function $I(a)$ too depends on $g(\boldsymbol{x})$.

MC algorithm. We now describe our numerical algorithm for the efficient MC simulation of unusual values of A for noninvertible maps $f(\boldsymbol{x})$. An alternative, statistically equivalent method for generating random sequence realizations, in the form of a Markov chain, is by first randomly sampling $\boldsymbol{x}_N$ from the IM $p_s(\boldsymbol{x})$ and then *stochastically* generating the elements of the sequence in reverse order by choosing $\boldsymbol{x}_i$ from the set $z\in f^{-1}(\boldsymbol{x}_{i+1})$ with probabilities $p_s(z)/[p_s(\boldsymbol{x}_{i+1})|J_f(z)|]$ [74]. Such reverse simulations have been employed successfully before (see, e.g., Ref. [65]). Importantly, they involve stochasticity, and therefore they enable one to *bias* the simulations, by choosing from among the preimages with probabilities that are different to those given above [65], a principle that we exploit in order to bias our simulations toward atypical values of A. Let us demonstrate this by considering the particularly simple case of $d = 1$, and assume that every x has exactly two preimages z_1, z_2, with $p_s(z_1)/|f'(z_1)| = p_s(z_2)/|f'(z_2)|$, as is the case for each of the doubling, tent, and logistic maps considered below. We define N indicator random variables $\xi_1,\dots,\xi_N$, where $\xi_i = 1$ (0) if x_i is the larger (smaller) of the two preimages of $f(x_i)$. From the definition of the stochastic reverse process, the ξ_i's are independent and identically distributed Bernoulli random variables with $\mathbb{P}(\xi_i = 0) = \mathbb{P}(\xi_i = 1) = 1/2$, and as a result, their sum $B = \sum_{i=1}^{N}\xi_i$ is binomially distributed, $\mathbb{P}(B = b) = \binom{N}{b}2^{-N}$. Using the law of total probability, we have

$$P(A=a) = \sum_{b=0}^{N} P(A=a\,|\,B=b)\mathbb{P}(B=b). \tag{6}$$

The reverse process can be simulated conditioned on B taking a specified value b, by (i) randomly choosing a subset $\mathcal{I}\subset\{1,\dots,N\}$ of size b [each subset is chosen with the same probability $\binom{N}{b}^{-1}$], (ii) randomly sampling a number x_{N+1} from the IM, and (iii) calculating $x_1,\dots,x_N$ in reverse order, where x_i is given by the larger (smaller) preimage of x_{i+1} if $i\in\mathcal{I}$ ($i\notin\mathcal{I}$). One then computes $P(A=a\,|\,B=b)$ from MC simulations of these restricted dynamics. Repeating this process for $b = 0,1,\dots,N$, one then computes $P(A=a)$ from Eq. (6). Atypical values of A are thus accessed, if they tend to occur concurrently with atypical values of B.

Applications. We now apply these tools to study several standard chaotic maps, beginning with the doubling map $f(x) = 2x \bmod 1$, where $x\in[0,1]$ and $z \bmod 1$ is the fractional part of z, with $g(x) = x$. Here, $f^{-1}(x) = \{x/2, (x+1)/2\}$, so Eq. (5) reads

$$\frac{e^{kx}}{2}\left[\psi\left(\frac{x}{2}\right) + \psi\left(\frac{x+1}{2}\right)\right] = e^{\lambda(k)}\psi(x), \tag{7}$$

whose solution,

$$\psi(x) = e^{2kx}, \quad \lambda(k) = \ln[(1+e^k)/2], \tag{8}$$

gives the rate function through a Legendre transform [75,76],

$$I(a) = a\ln a + (1-a)\ln(1-a) + \ln 2. \quad (9)$$

As the reader may have noticed, $I(a)$ is precisely the rate function that describes a binomial distribution (see, e.g., Ref. [43]). We explain this coincidence in the Supplemental Material (SM) [74] by calculating $I(a)$ via an alternative method, providing a validation of (9).

Let us now consider the tent map, $f(x) = 1 - |1-2x|$, again with $g(x) = x$. Before turning to the calculation of $I(a)$, we make two observations: (i) As we find in the SM [74], A is strictly bounded from above by $m_N = \max_{x_1\in[0,1]} \mathcal{A}(x_1)$ which, at $N\to\infty$, converges to $m_\infty = 2/3$, the nontrivial fixed point of $f(x)$. We therefore anticipate that the support of $I(a)$ is the interval $[0, 2/3]$, which, as shown below, is indeed the case. This is nontrivial, since the IM for the tent map is uniform over the entire interval [0,1). (ii) If $x_1 \sim 2^{-N}$, then $A \sim 1/N$. The probability for this is $\sim 2^{-N}$, which, using (2), leads to the bound $I(0) \leqslant \ln 2$. Similarly, if $|x_1 - 2/3| \sim 2^{-N}$ then $|A - 2/3| \sim 1/N$, leading to $I(2/3) \leqslant \ln 2$. In fact, we find below that these inequalities are saturated, $I(0) = I(2/3) = \ln 2$.

Let us calculate $I(a)$. For the tent map, Eq. (5) reads

$$\tilde{L}_k\psi(x) = \frac{e^{kx}}{2}\left[\psi\left(\frac{x}{2}\right) + \psi\left(1-\frac{x}{2}\right)\right] = e^{\lambda(k)}\psi(x). \quad (10)$$

We now present an exact solution to Eq. (10), which we obtain in the form of a perturbation theory in k that can be exactly solved at all orders. The IM $p_s(x)$ is uniform over $x \in [0, 1)$, and indeed, one finds that for $k = 0$, $\psi(x) = 1$ and $\lambda(k) = 0$. We expand in k,

$$\psi(x) = 1 + k\psi_1(x) + k^2\psi_2(x) + \cdots, \quad (11)$$

$$\lambda(k) = k\lambda_1 + k^2\lambda_2 + \cdots. \quad (12)$$

Let us first find the solution to first order in k. Keeping terms up to order $O(k)$ in Eq. (10), we obtain

$$1 + \frac{k}{2}\left[2x + \psi_1\left(\frac{x}{2}\right) + \psi_1\left(1-\frac{x}{2}\right)\right] = 1 + k[\lambda_1 + \psi_1(x)], \quad (13)$$

whose exact solution is $\psi_1(x) = x$, $\lambda_1 = 1/2$. This perturbative procedure can be explicitly carried out to arbitrary order in k, yielding the exact rate function $I(a)$. $\psi_n(x)$ turns out to be a polynomial of degree n, whose coefficients are found by solving a set of linear equations. In the SM [74], we work out the leading orders explicitly, and obtain

$$\lambda(k) = \frac{k}{2} + \frac{k^2}{24} - \frac{k^3}{72} + \frac{41k^4}{8640} + \cdots, \quad (14)$$

whose Legendre transform is

$$I(a) = 6\left(a-\tfrac{1}{2}\right)^2 + 24\left(a-\tfrac{1}{2}\right)^3 + \tfrac{588}{5}\left(a-\tfrac{1}{2}\right)^4 + \cdots. \quad (15)$$

We give the solution up to eighth order in the SM [74].

We now consider the logistic map [77] at the Ulam point, $f(x) = 4x(1-x)$, where $x \in [0, 1)$, with $g(x) = x$. The analysis is very similar to that of the tent map [74]. This time, the support of $I(a)$ is $[0, 3/4]$, $x = 3/4$ being a fixed point of $f(x)$, with $I(0) = I(3/4) = \ln 2$, and Eq. (5) reads

$$\tilde{L}_k\psi(x) = \frac{e^{kx}\left[\psi\left(\frac{1+\sqrt{1-x}}{2}\right) + \psi\left(\frac{1-\sqrt{1-x}}{2}\right)\right]}{4\sqrt{1-x}} = e^{\lambda(k)}\psi(x). \quad (16)$$

As in the tent map, we solve Eq. (16) perturbatively in k to arbitrary order. Expanding

$$\psi(x) = p_s(x)[1 + k\psi_1(x) + k^2\psi_2(x) + \cdots], \quad (17)$$

where $p_s(x) = [\pi\sqrt{x(1-x)}]^{-1}$ is the IM [78], and $\lambda(k) = k\lambda_1 + k^2\lambda_2 + \cdots$, we again find that $\psi_n(x)$ is a polynomial of degree n whose coefficients can be found explicitly. In the SM [74] we find

$$\lambda(k) = \frac{k}{2} + \frac{k^2}{16} - \frac{k^3}{64} + \frac{3k^4}{1024} + \cdots, \quad (18)$$

whose Legendre transform is

$$I(a) = 4\left(a-\tfrac{1}{2}\right)^2 + 8\left(a-\tfrac{1}{2}\right)^3 + 24\left(a-\tfrac{1}{2}\right)^4 + \cdots. \quad (19)$$

The solution up to sixth order is found in the SM [74]. As shown in Fig. 1, Eqs. (15) and (19) are in excellent agreement with numerical computations of $P(A = a)$ from biased MC simulations with $N = 50$, and with semianalytic calculations of $I(a)$ obtained by computing the largest eigenvalue $e^{\lambda(k)}$ of $\tilde{L}_k$ numerically using Ulam discretization [79], and then performing the Legendre transform numerically. Also plotted are the asymptotic behaviors of the rate functions near the edges of their supports, which we obtain in the SM [74] by solving the eigenvalue problems in the limits $k \to \pm\infty$. Before moving on, we note that for the doubling, tent, and logistic maps, $I(a) = \ln 2$—which, in all these systems, equals the Lyapunov exponent—at the edges of its support. We speculate that this feature may be universal for $d = 1$.

We now turn to Arnold's cat map, where we uncover strong numerical evidence pointing at the existence of a remarkable DPT in $I(a)$. Here, $d = 2$, and $\boldsymbol{x}_i = (y_i, z_i) \in [0, 1] \times [0, 1]$. The cat map is defined by

$$f(y, z) = [(y+z) \bmod 1, (y+2z) \bmod 1]. \quad (20)$$

Its IM is uniform on the unit square. We consider $g(y, z) = (y+z)/2$ [80]. $f(y, z)$ is invertible, with $|J_f(y, z)| = 1$, so Eq. (5) becomes

$$e^{k(y+z)/2}\psi[(2y-z) \bmod 1, (z-y) \bmod 1] = e^{\lambda(k)}\psi(y, z). \quad (21)$$

Equation (21) proved difficult to solve analytically or even numerically, because of instabilities of the Ulam method (that occur even for $k = 0$ [63,81]). Though we did not solve Eq. (21), we are nevertheless able to predict some features of $I(a)$ by making the following observations: (i) The dynamics are statistically invariant under the transformation $(y_i, z_i) \to (1-y_i, 1-z_i)$. Therefore, $P(A = a) = P(A = 1-a)$ is exactly symmetric, implying $I(a) = I(1-a)$. (ii) One can check that the joint distribution of any pair (ξ_1, ξ_2) of distinct elements taken from the set $\{y_1, z_1, \ldots, y_N, z_N\}$ is uniform on the unit square, implying that ξ_1, ξ_2 are statistically independent. Therefore, using $\langle y_i\rangle = \langle z_i\rangle = 1/2$ and $\operatorname{Var} y_i = \operatorname{Var} z_i =$

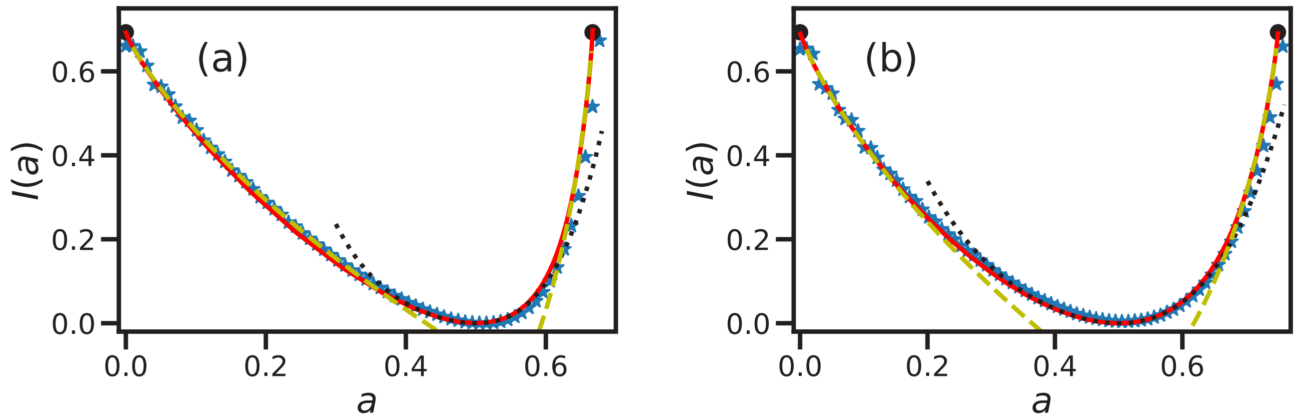

FIG. 1. Rate functions $I(a)$ that describe the full distributions $P(A = a)$ at $N \gg 1$ for the tent map (a) and logistic map (b). Solid lines were obtained through numerical diagonalizations of $\tilde{L}_k$ from Eqs. (10) and (16), respectively. Dotted lines are the exact analytic solutions, evaluated up to order $O[(a - 1/2)^4]$, Eqs. (15) and (19), respectively. Markers correspond to properly rescaled data from biased MC simulations with $N = 50$ (see SM [74] for details). The points $I(0) = I(2/3) = \ln 2$ in (a) and $I(0) = I(3/4) = \ln 2$ in (b) are marked by •. Dashed lines correspond to the asymptotic behaviors of the rate functions near the edges of their supports, that we calculate in the SM [74].

$1/12$, we find $\langle A \rangle = 1/2$ and $\operatorname{Var} A = 1/(24N)$ so, using (2), we anticipate the parabolic behavior

$$I(a) = 12(a - 1/2)^2 + o[(a - 1/2)^2], \tag{22}$$

corresponding to a Gaussian distribution of typical fluctuations as described by (an extension of) the central limit theorem. (iii) The Lyapunov exponents of the cat map are $\pm 2 \ln \varphi$, where $\varphi = (1 + \sqrt{5})/2 = 1.618\ldots$ is the golden ratio. Therefore, if $y_1, z_1 \sim \varphi^{-2N}$, then the elements of the sequence grow with i as $y_i, z_i \sim \varphi^{2i-2N}$, and as a result, $A \sim 1/N$. The probability for this is $\sim \varphi^{-4N}$, leading to the bound $I(0) \leqslant 4 \ln \varphi = 1.9248\ldots$ and similarly for $I(1)$.

In Fig. 2(a), we plot $I(a)$, which we computed from direct MC simulations with $N = 10$ (since the cat map is invertible, we could not use the algorithm introduced in this work, and had to resort to direct MC simulations instead). Good agreement with the prediction of Eq. (22) is observed at $a \simeq 1/2$. In addition, we found that the bounds given above for $a = 0$ and $a = 1$ are in fact saturated, $I(0) = I(1) = 4 \ln \varphi$.

Far more remarkable, however, $I(a)$ appears to behave *exactly* linearly for $a \in [0, a_c]$ with $a_c \simeq 0.3$ [due to the symmetry $I(a) = I(1 - a)$, this occurs symmetrically at $a \in [1 - a_c, 1]$ too). This is seen more clearly in Fig. 2(b), where $I'(a)$ is plotted. Indeed, $I'(a)$ appears to have a corner singularity at $a = a_c$, and to take a constant value $I'(a) \simeq -4.7$ for $a \in [0, a_c]$. In the distribution (2), $I(a)$ assumes the role of an effective free energy, and we therefore interpret this singularity as a second-order DPT, because $I(a)$ and $I'(a)$ are continuous at the transition, but $I''(a)$ jumps [82]. This (apparent) DPT constitutes a central result of this Letter. At $a \in [0, a_c]$, we expect the system to display coexistence between the $a = 0$ and $a = a_c$ states, meaning that for a fraction a/a_c $(1 - a/a_c)$ of the dynamics, the system will display the statistical behavior that corresponds to $a = 0$ $(a = a_c)$. In particular, we expect the distribution $P(x|A = a)$ of each element in the sequence, conditioned on observing a given $A = a \in [0, a_c]$, to be given by the superposition

$$P(x|A = a) = \left(1 - \frac{a}{a_c}\right) P(x|A = 0) + \frac{a}{a_c} P(x|A = a_c) \tag{23}$$

of the corresponding distributions conditioned on observing $A = 0$ and $A = a_c$, respectively. This interpretation draws an

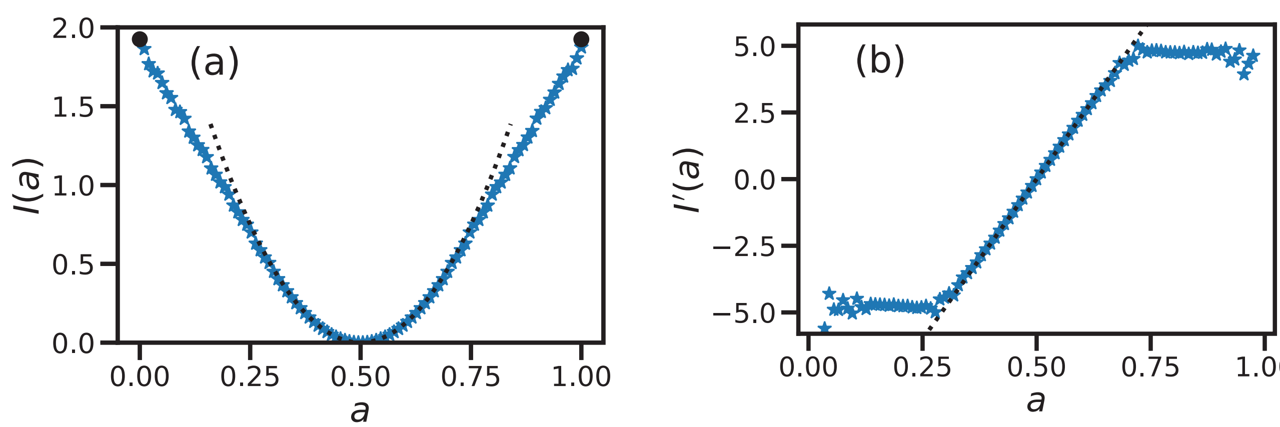

FIG. 2. (a) Markers correspond to data from 2×10^{10} direct MC simulations with $N = 10$ for the cat map [74], showing good agreement with the prediction (22) (dotted line) at $a \simeq 1/2$. The points $I(0) = I(1) = 4 \ln \varphi$ are marked by •. (b) $I'(a)$, showing a corner singularity (second-order DPT) at $a = a_c$ and $a = 1 - a_c$, and taking constant values at $a \in [0, a_c]$ and at $a \in [1 - a_c, 1]$.

analogy to DPTs that were found in stochastic systems (see, e.g., Refs. [37,38,40]).

Discussion. We studied dynamical observables in the doubling, tent, logistic, and cat maps. By using an existing theoretical framework [27,55,66,67], we calculated the rate functions exactly (for particular observables) in the former three maps, where for the tent and logistic maps, our result is given in the form of a perturbation theory that can be solved to all orders. Moreover, we calculated the rate function numerically for the cat map. The rate functions $I(a)$ that we found have interesting properties: (i) For the tent and logistic maps, the rate functions are asymmetric although the IMs are symmetric, and in fact even the rate functions' supports differ from those of the IMs. (ii) In all of the cases studied here, the supports of the rate functions are related to fixed points of the map $f(\boldsymbol{x})$, and at the edges of their supports, the rate functions take values that are related to the system's Lyapunov exponents. (iii) For the cat map, $I(a)$ has a remarkable singularity that we interpret as a second-order DPT, causing unusual values of A to be far likelier than one would expect by extrapolating from the central part of the distribution. It would be interesting to extend our results to other maps and/or to other observables.

As an alternative approach to ours, one could characterize the set of initial conditions x_1 for which $\mathcal{A}(x_1) = a$, since the statistical weight of this set (according to the IM) gives $P(A = a)$. In the limit $N \to \infty$, this set becomes

$$S_a = \left\{ x_1 | \lim_{N\to\infty} \frac{1}{N} \sum_{n=0}^{N-1} g[f^{(n)}(x_1)] = a \right\}. \qquad (24)$$

For instance, for $f(x) =$ the doubling map and $g(x) = x$, S_a is the set of numbers $x_1 \in [0, 1]$ whose binary representation has a ratio of $1 - a : a$ between zeros and ones [74]. One could then explore possible connections between our rate function $I(a)$ and various fractal dimensions of S_a (see Refs. [66,67,83–87] where fractal dimensions were studied, and in particular, phase transitions were found [66,83,84]).

Finally, in some stochastic systems, the scaling (2) was recently found to break down and give way to anomalous scalings of large deviations [88–98] or of the distributions' cumulants [99,100]. It would be interesting to search for anomalous scalings in deterministic, chaotic systems.

Acknowledgments. I thank Satya N. Majumdar and Grégory Schehr for pointing out useful references, Roiy Sayag and Tal Agranov for their comments on the manuscript, and Domenico Lippolis for a very helpful correspondence concerning eigenvalues of the Frobenius-Perron operator in the cat map.

[1] T. Geisel and J. Nierwetberg, Onset of Diffusion and Universal Scaling in Chaotic Systems, Phys. Rev. Lett. **48**, 7 (1982).

[2] M. Schell, S. Fraser, and R. Kapral, Diffusive dynamics in systems with translational symmetry: A one-dimensional-map model, Phys. Rev. A **26**, 504 (1982).

[3] H. Fujisaka and S. Grossmann, Chaos-induced diffusion in nonlinear discrete dynamics, Z. Phys. B **48**, 261 (1982).

[4] Y. Sato and R. Klages, Anomalous Diffusion in Random Dynamical Systems, Phys. Rev. Lett. **122**, 174101 (2019).

[5] T. Albers, D. Müller-Bender, and G. Radons, Antipersistent random walks in time-delayed systems, Phys. Rev. E **105**, 064212 (2022).

[6] J. Wouters and F. Bouchet, Rare event computation in deterministic chaotic systems using genealogical particle analysis, J. Phys. A: Math. Theor. **49**, 374002 (2016).

[7] F. Ragone, J. Wouters, and F. Bouchet, Computation of extreme heat waves in climate models using a large deviation algorithm, Proc. Natl. Acad. Sci. USA **115**, 24 (2018).

[8] F. Ragone and F. Bouchet, Rare event algorithm study of extreme warm summers and heatwaves over Europe, Geophys. Res. Lett. **48**, e2020GL091197 (2021).

[9] B.-W. Shen, R. A. Pielke Sr., X. Zeng, J.-J. Baik, S. Faghih-Naini, J. Cui, and R. Atlas, Is weather chaotic?: Coexistence of chaos and order within a generalized Lorenz model, Bull. Am. Meteorol. Soc. **102**, 148 (2021).

[10] V. M. Gálfi, V. Lucarini, F. Ragone, and J. Wouters, Applications of large deviation theory in geophysical fluid dynamics and climate science, Riv. Nuovo Cimento **44**, 291 (2021).

[11] V. M. Galfi and V. Lucarini, Fingerprinting Heatwaves and Cold Spells and Assessing Their Response to Climate Change Using Large Deviation Theory, Phys. Rev. Lett. **127**, 058701 (2021).

[12] M. d'Errico, F. Pons, P. Yiou, S. Tao, C. Nardini, F. Lunkeit, and D. Faranda, Present and future synoptic circulation patterns associated with cold and snowy spells over Italy, Earth Syst. Dynam. **13**, 961 (2022).

[13] I. Klioutchnikova, M. Sigovaa, and N. Beizerov, Chaos theory in finance, Procedia Comput. Sci. **119**, 368 (2017).

[14] L. A. Safonova, E. Tomer, V. V. Strygin, Y. Ashkenazy, and S. Havlin, Multifractal chaotic attractors in a system of delay-differential equations modeling road traffic, Chaos **12**, 1006 (2002).

[15] F. Roy, G. Biroli, G. Bunin, and C. Cammarota, Numerical implementation of dynamical mean field theory for disordered systems: application to the Lotka-Volterra model of ecosystems, J. Phys. A: Math. Theor. **52**, 484001 (2019).

[16] F. Roy, M. Barbier, G. Biroli, and G. Bunin, Complex interactions can create persistent fluctuations in high-diversity ecosystems, PLoS Comput. Biol. **16**, e1007827 (2020).

[17] M. T. Pearce, A. Agarwala, and D. S. Fisher, Stabilization of extensive fine-scale diversity by ecologically driven spatiotemporal chaos, Proc. Natl. Acad. Sci. USA **117**, 14572 (2020).

[18] O. Postavaru, S. R. Anton, and A. Toma, COVID-19 pandemic and chaos theory, Math. Comput. Simul. **181**, 138 (2021).

[19] S. S. Varadhan, *Large Deviations and Applications*, CBMS-NSF Regional Conference Series in Applied Mathematics No. 46 (SIAM, Philadelphia, 1984).

[20] Y. Oono, Prog. Theor. Phys. Suppl. **99**, 165 (1989).

[21] A. Dembo and O. Zeitouni, *Large Deviations Techniques and Applications*, 2nd ed. (Springer, New York, 1998).

[22] F. den Hollander, *Large Deviations*, Fields Institute Monographs Vol. 14 (AMS, Providence, RI, 2000).

[23] S. N. Majumdar and A. J. Bray, Large-deviation functions for nonlinear functionals of a Gaussian stationary Markov process, Phys. Rev. E **65**, 051112 (2002).
[24] J. A. Bucklew, *Introduction to Rare Event Simulation* (Springer, New York, 2004).
[25] S. N. Majumdar, Brownian functionals in physics and computer science, Curr. Sci. **89**, 93 (2006).
[26] B. Derrida, Non-equilibrium steady states: fluctuations and large deviations of the density and of the current, J. Stat. Mech.: Theory Exp. (2007) P07023.
[27] H. Touchette, The large deviation approach to statistical mechanics, Phys. Rep. **478**, 1 (2009).
[28] B. Waclaw, R. J. Allen, and M. R. Evans, Dynamical Phase Transition in a Model for Evolution with Migration, Phys. Rev. Lett. **105**, 268101 (2010).
[29] B. Derrida, Microscopic versus macroscopic approaches to non-equilibrium systems, J. Stat. Mech.: Theory Exp. (2011) P01030.
[30] H. Touchette, A basic introduction to large deviations: Theory, applications, simulations, in *Modern Computational Science 11: Lecture Notes from the 3rd International Oldenburg Summer School*, edited by R. Leidl and A. K. Hartmann (BIS-Verlag der Carl von Ossietzky, Universität Oldenburg, 2011).
[31] O. Cohen and D. Mukamel, Phase Diagram and Density Large Deviations of a Nonconserving *ABC* Model, Phys. Rev. Lett. **108**, 060602 (2012).
[32] J. Szavits-Nossan, M. R. Evans, and S. N. Majumdar, Constraint-Driven Condensation in Large Fluctuations of Linear Statistics, Phys. Rev. Lett. **112**, 020602 (2014).
[33] L. Bertini, A. De Sole, D. Gabrielli, G. Jona-Lasinio, and C. Landim, Macroscopic fluctuation theory, Rev. Mod. Phys. **87**, 593 (2015).
[34] B. Meerson and S. Redner, Mortality, Redundancy, and Diversity in Stochastic Search, Phys. Rev. Lett. **114**, 198101 (2015).
[35] P. Vivo, Large deviations of the maximum of independent and identically distributed random variables, Eur. J. Phys. **36**, 055037 (2015).
[36] Y. Baek and Y. Kafri, Singularities in large deviation functions, J. Stat. Mech.: Theory Exp. (2015) P08026.
[37] Y. Baek, Y. Kafri, and V. Lecomte, Dynamical Symmetry Breaking and Phase Transitions in Driven Diffusive Systems, Phys. Rev. Lett. **118**, 030604 (2017).
[38] Y. Baek, Y. Kafri, and V. Lecomte, Dynamical phase transitions in the current distribution of driven diffusive channels, J. Phys. A: Math. Theor. **51**, 105001 (2018).
[39] O. Shpielberg and E. Akkermans, Le Chatelier Principle for Out-of-Equilibrium and Boundary-Driven Systems: Application to Dynamical Phase Transitions, Phys. Rev. Lett. **116**, 240603 (2016).
[40] P. Tsobgni Nyawo and H. Touchette, A minimal model of dynamical phase transition, Europhys. Lett. **116**, 50009 (2016).
[41] A. Krajenbrink and P. Le Doussal, Exact short-time height distribution in the one-dimensional Kardar-Parisi-Zhang equation with Brownian initial condition, Phys. Rev. E **96**, 020102(R) (2017).
[42] M. Assaf and B. Meerson, WKB theory of large deviations in stochastic populations, J. Phys. A: Math. Theor. **50**, 263001 (2017).
[43] S. N. Majumdar and G. Schehr, Large deviations, ICTS Newsletter **3** (2) (2017), https://www.icts.res.in/sites/default/files/newsletter-2017-vol-3-issue-2.pdf
[44] H. Touchette, Introduction to dynamical large deviations of Markov processes, Physica A **504**, 5 (2018).
[45] N. R. Smith, A. Kamenev, and B. Meerson, Landau theory of the short-time dynamical phase transitions of the Kardar-Parisi-Zhang interface, Phys. Rev. E **97**, 042130 (2018).
[46] A. K. Hartmann, Sampling rare events: Statistics of local sequence alignments, Phys. Rev. E **65**, 056102 (2002).
[47] L.-S. Young, Some large deviation results for dynamical systems, Trans. Am. Math. Soc. **318**, 525 (1990).
[48] F. M. Cucchietti, C. H. Lewenkopf, E. R. Mucciolo, H. M. Pastawski, and R. O. Vallejos, Measuring the Lyapunov exponent using quantum mechanics, Phys. Rev. E **65**, 046209 (2002).
[49] G. Haller, Distinguished material surfaces and coherent structures in three-dimensional fluid flows, Physica D **149**, 248 (2001).
[50] G. Haller, An objective definition of a vortex, J. Fluid Mech. **525**, 1 (2005).
[51] J.-P. Eckmann and I. Procaccia, Fluctuations of dynamical scaling indices in nonlinear systems, Phys. Rev. A **34**, 659 (1986).
[52] G. Paladin and A. Vulpiani, Anomalous scaling laws in multifractal objects, Phys. Rep. **156**, 147 (1987).
[53] U. Frisch, *Turbulence, The Legacy of A. N. Kolmogorov* (Cambridge University Press, Cambridge, UK, 1995).
[54] J. Bec, Lyapunov exponents of heavy particles in turbulence, Phys. Fluids **18**, 091702 (2006).
[55] R. Aimino and S. Vaienti, A note on the large deviations for piecewise expanding multidimensional maps, in *Nonlinear Dynamics New Directions. Nonlinear Systems and Complexity*, edited by H. González-Aguilar and E. Ugalde, Series on Mathematical Method and Modeling Vol. 11 (Springer, Cham, 2015), pp. 1–10.
[56] T. Laffargue, K.-D. Nguyen Thu Lam, J. Kurchan, and J. Tailleur, Large deviations of Lyapunov exponents, J. Phys. A: Math. Theor. **46**, 254002 (2013).
[57] L. Biferale, C. Meneveau, and R. Verzicco, Deformation statistics of sub-Kolmogorov-scale ellipsoidal neutrally buoyant drops in isotropic turbulence, J. Fluid Mech. **754**, 184 (2014).
[58] J. C. Leitão, J. M. Viana Parente Lopes, and E. G. Altmann, Efficiency of Monte Carlo sampling in chaotic systems, Phys. Rev. E **90**, 052916 (2014).
[59] P. L. Johnson and C. Meneveau, Large-deviation joint statistics of the finite-time Lyapunov spectrum in isotropic turbulence, Phys. Fluids **27**, 085110 (2015).
[60] D. Pazó, J. M. López, and A. Politi, Diverging Fluctuations of the Lyapunov Exponents, Phys. Rev. Lett. **117**, 034101 (2016).
[61] J. C. Leitão, J. M. Viana Parente Lopes, and E. G. Altmann, Importance sampling of rare events in chaotic systems, Eur. Phys. J. B **90**, 181 (2017).
[62] L. De Cruz, S. Schubert, J. Demaeyer, V. Lucarini, and S. Vannitsem, Exploring the Lyapunov instability properties of high-dimensional atmospheric and climate models, Nonlinear Process. Geophys. **25**, 387 (2018).
[63] K. Yoshida, H. Yoshino, A. Shudo, and D. Lippolis, Eigenfunctions of the Perron-Frobenius operator and the finite-time

Lyapunov exponents in uniformly hyperbolic area-preserving maps, J. Phys. A: Math. Theor. **54**, 285701 (2021).
[64] C. Anteneodo, S. Camargo, and R. O. Vallejos, Importance sampling with imperfect cloning for the computation of generalized Lyapunov exponents, Phys. Rev. E **96**, 062209 (2017).
[65] P. Grassberger, Information flow and maximum entropy measures for 1-D maps, Physica D **14**, 365 (1985).
[66] P. Grassberger, R. Badii, and A. Politi, Scaling laws for invariant measures on hyperbolic and nonhyperbolic atractors, J. Stat. Phys. **51**, 135 (1988).
[67] G. Parisi, Appendix, in U. Frisch, Fully developed turbulence and intermittency, in *Proceedings of International School on Turbulence and Predictability in Geophysical Fluid Dynamics and Climate Dynamics*, edited by M. Ghil (North-Holland, Amsterdam, 1984).
[68] C. Beck and F. Schlögl, *Thermodynamics of Chaotic Systems* (Cambridge University Press, Cambridge, UK, 1993).
[69] C. Anteneodo, Statistics of finite-time Lyapunov exponents in the Ulam map, Phys. Rev. E **69**, 016207 (2004).
[70] For brevity, we denote the probability density function (PDF) of A by $P(A = a)$.
[71] It is well known that some of the chaotic maps considered in this Letter are homeomorphic to each other: A sequence $x_1, x_2, \dots$ generated by a chaotic map $x_{i+1} = f(x_i)$, can be transformed to a sequence $\tilde{x}_i = h(x_i)$ that is generated by some other chaotic map, i.e., $\tilde{x}_{i+1} = \tilde{f}(\tilde{x}_i)$. In particular, this is the case for $f(x) =$ the tent map, and $\tilde{f}(\tilde{x}) =$ the logistic map, with $h(x) = \sin^2(\pi x/2)$ [72]. However, note that in the context of the present Letter, applying such a transformation $h(x)$ would affect the observable via $g(x)$.
[72] https://en.wikipedia.org/wiki/Tent_map
[73] J. Gärtner, On large deviations from the invariant measure, Theory Probab. Appl. **22**, 24 (1977); R. S. Ellis, Large deviations for a general class of random vectors, Ann. Prob. **12**, 1 (1984).
[74] See Supplemental Material at http://link.aps.org/supplemental/10.1103/PhysRevE.106.L042202, which includes Refs. [101–108].
[75] Since $\lambda(k)$ is differentiable and strictly convex, the Legendre-Fenchel transform reduces to a Legendre transform [76], which, for Eq. (8) yields $I(a)$ via $a = \lambda'(k) = \frac{e^k}{1+e^k}$, leading to $k = \ln \frac{a}{1-a}$ which is plugged into $I = ka - \lambda(k)$ to obtain Eq. (9).
[76] H. Touchette, Legendre-Fenchel transforms in a nutshell, https://www.ise.ncsu.edu/fuzzy-neural/wp-content/uploads/sites/9/2019/01/or706-LF-transform-1.pdf (2005).
[77] M. J. Feigenbaum, Quantitative universality for a class of nonlinear transformations, J. Stat. Phys. **19**, 25 (1978).
[78] S. Ulam and J. von Neumann, On combination of stochastic and deterministic processes, Bull. Am. Math. Soc. **53**, 1120 (1947).
[79] S. Klus, P. Koltai, and C. Schütte, On the numerical approximation of the Perron-Frobenius and Koopman operator, J. Comput. Dyn. **3**, 51 (2016).
[80] Equivalently, one can define A to be the series $A = (\sum_{i=1}^{2N} w_i)/(2N)$, where (w_1, w_2) are sampled uniformly from the unit square, and $w_{i+1} = (w_i + w_{i-1}) \bmod 1$.
[81] F. Brini, S. Siboni, G. Turchetti, and S. Vaienti, Decay of correlations for the automorphism of the torus $\mathbb{T}^2$, Nonlinearity **10**, 1257 (1997).
[82] However, analogous transitions for stochastic systems have been categorized as first order [40].
[83] E. Ott, W. D. Withers, and J. A. Yorke, Is the dimension of chaotic attractors invariant under coordinate changes? J. Stat. Phys. **36**, 687 (1984).
[84] D. Katzen and I. Procaccia, Phase Transitions in the Thermodynamic Formalism of Multifractals, Phys. Rev. Lett. **58**, 1169 (1987).
[85] U. Frisch, Ou en est la Turbulence Developpée? Phys. Scr. **T9**, 137 (1985).
[86] R. Benzi, G. Paladin, G. Parisi, and A. Vulpiani, On the multifractal nature of fully developed turbulence and chaotic systems, J. Phys. A: Math. Gen. **17**, 3521 (1984).
[87] M. H. Jensen, L. P. Kadanoff, A. Libchaber, I. Procaccia, and J. Stavans, Global Universality at the Onset of Chaos: Results of a Forced Rayleigh-Bénard Experiment, Phys. Rev. Lett. **55**, 2798 (1985); T. C. Halsey, M. H. Jensen, L. P. Kadanoff, I. Procaccia, and B. I. Shraiman, Fractal measures and their singularities: The characterization of strange sets, Phys. Rev. A **33**, 1141 (1986).
[88] D. Nickelsen and H. Touchette, Anomalous Scaling of Dynamical Large Deviations, Phys. Rev. Lett. **121**, 090602 (2018).
[89] G. Gradenigo and S. N. Majumdar, A first-order dynamical transition in the displacement distribution of a driven run-and-tumble particle, J. Stat. Mech.: Theory Exp. (2019) 053206.
[90] B. Meerson, Anomalous scaling of dynamical large deviations of stationary Gaussian processes, Phys. Rev. E **100**, 042135 (2019).
[91] R. L. Jack and R. J. Harris, Giant leaps and long excursions: Fluctuation mechanisms in systems with long-range memory, Phys. Rev. E **102**, 012154 (2020).
[92] F. Brosset, T. Klein, A. Lagnoux, and P. Petit, Probabilistic proofs of large deviation results for sums of semiexponential random variables and explicit rate function at the transition, arXiv:2007.08164.
[93] G. Gradenigo, S. Iubini, R. Livi, and S. N. Majumdar, Localization transition in the discrete nonlinear Schrödinger equation: ensembles inequivalence and negative temperatures, J. Stat. Mech.: Theory Exp. (2021) 023201.
[94] G. Gradenigo, S. Iubini, R. Livi, and S. N. Majumdar, Condensation transition and ensemble inequivalence in the discrete nonlinear Schrödinger equation, Eur. Phys. J. E **44**, 29 (2021).
[95] F. Mori, P. Le Doussal, S. N. Majumdar, and G. Schehr, Condensation transition in the late-time position of a run-and-tumble particle, Phys. Rev. E **103**, 062134 (2021).
[96] F. Mori, G. Gradenigo, and S. N. Majumdar, First-order condensation transition in the position distribution of a run-and-tumble particle in one dimension, J. Stat. Mech.: Theory Exp. (2021) 103208.
[97] N. R. Smith, Anomalous scaling and first-order dynamical phase transition in large deviations of the Ornstein-Uhlenbeck process, Phys. Rev. E **105**, 014120 (2022).
[98] N. R. Smith and S. N. Majumdar, Condensation transition in large deviations of self-similar Gaussian processes with stochastic resetting, J. Stat. Mech.: Theory Exp. (2022) 053212.

[99] Ž. Krajnik, E. Ilievski, and T. Prosen, Absence of Normal Fluctuations in an Integrable Magnet, Phys. Rev. Lett. **128**, 090604 (2022).

[100] Ž. Krajnik, J. Schmidt, V. Pasquier, E. Ilievski, and T. Prosen, Exact Anomalous Current Fluctuations in a Deterministic Interacting Model, Phys. Rev. Lett. **128**, 160601 (2022).

[101] C. De Bacco, A. Guggiola, R. Kühn, and P. Paga, Rare events statistics of random walks on networks: localisation and other dynamical phase transitions, J. Phys. A: Math. Theor. **49**, 184003 (2016).

[102] P. Tsobgni Nyawo and H. Touchette, Large deviations of the current for driven periodic diffusions, Phys. Rev. E **94**, 032101 (2016).

[103] S. Whitelam, Large deviations in the presence of cooperativity and slow dynamics, Phys. Rev. E **97**, 062109 (2018).

[104] F. Coghi, J. Morand, and H. Touchette, Large deviations of random walks on random graphs, Phys. Rev. E **99**, 022137 (2019).

[105] R. Gutierrez and C. Perez-Espigares, Generalized optimal paths and weight distributions revealed through the large deviations of random walks on networks, Phys. Rev. E **103**, 022319 (2021).

[106] S. Whitelam and D. Jacobson, Varied phenomenology of models displaying dynamical large-deviation singularities, Phys. Rev. E **103**, 032152 (2021).

[107] G. Carugno, P. Vivo, and F. Coghi, Graph-combinatorial approach for large deviations of Markov chains, J. Phys. A: Math. Theor. **55**, 295001 (2022).

[108] C. Monthus, Markov trajectories: Microcanonical ensembles based on empirical observables as compared to canonical ensembles based on Markov generators, Eur. Phys. J. B **95**, 139 (2022).